Supplementary Figures and Figure legends

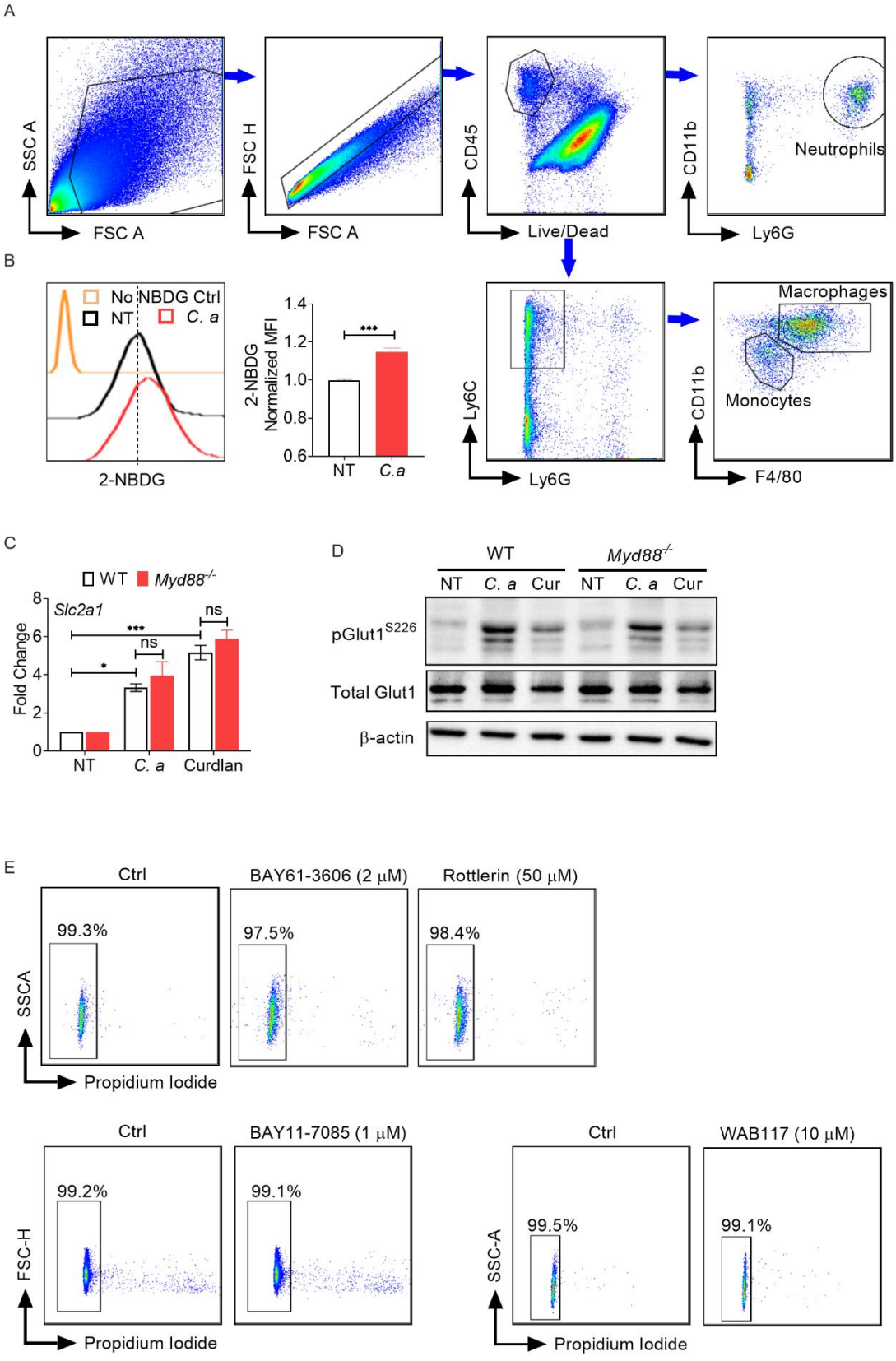

Fig S1: Increased glucose uptake by fungal-stimulated neutrophils. **(A)** Representative flow cytometry analysis gating strategy for identification of kidney infiltrating immune cells: neutrophils (liveCD45^{+}CD11b^{+}Ly6G^{+}), macrophages (liveCD45^{+}Ly6C^{+}Ly6G^{-}CD11b^{hi}F4/80^{hi}), monocytes (liveCD45^{+}Ly6C^{+}Ly6G^{-}CD11b^{low}F4/80^{low}). **(B)** BM neutrophils from WT mice were stimulated with *C. a* (MOI=1) for 1.5 h. Glucose uptake by neutrophils was detected by flow cytometry analysis using a fluorescent glucose analog 2-NBDG. **(C)** Neutrophils from WT or *Myd88*$^{-/-}$ mice were stimulated with *C. a* (MOI=0.2) or curdlan (10 μg/ml). Gene expression of *Slc2a1* was assessed by qPCR. **(D)** Neutrophils from WT or *Myd88*$^{-/-}$ mice were stimulated with *C. a* (MOI=1) or curdlan (100 μg/ml). Phosphorylation of Glut1 was measured by western blot at 30 min post-stimulation. **(E)** Neutrophils from WT mice were either treated with indicated inhibitors for 3 h or left untreated (Ctrl). Cells were stained by Propidium Iodide and assessed for viability by flow cytometry analysis. Data pooled from at least 3 independent experiments (A-C) and representative images from 3 experiments (D) are shown. Statistical analysis by Student's T test (B) and Two-way ANOVA (C). Data are represented as mean ± SEM (B, C). (Related to Figure 1 and 2)

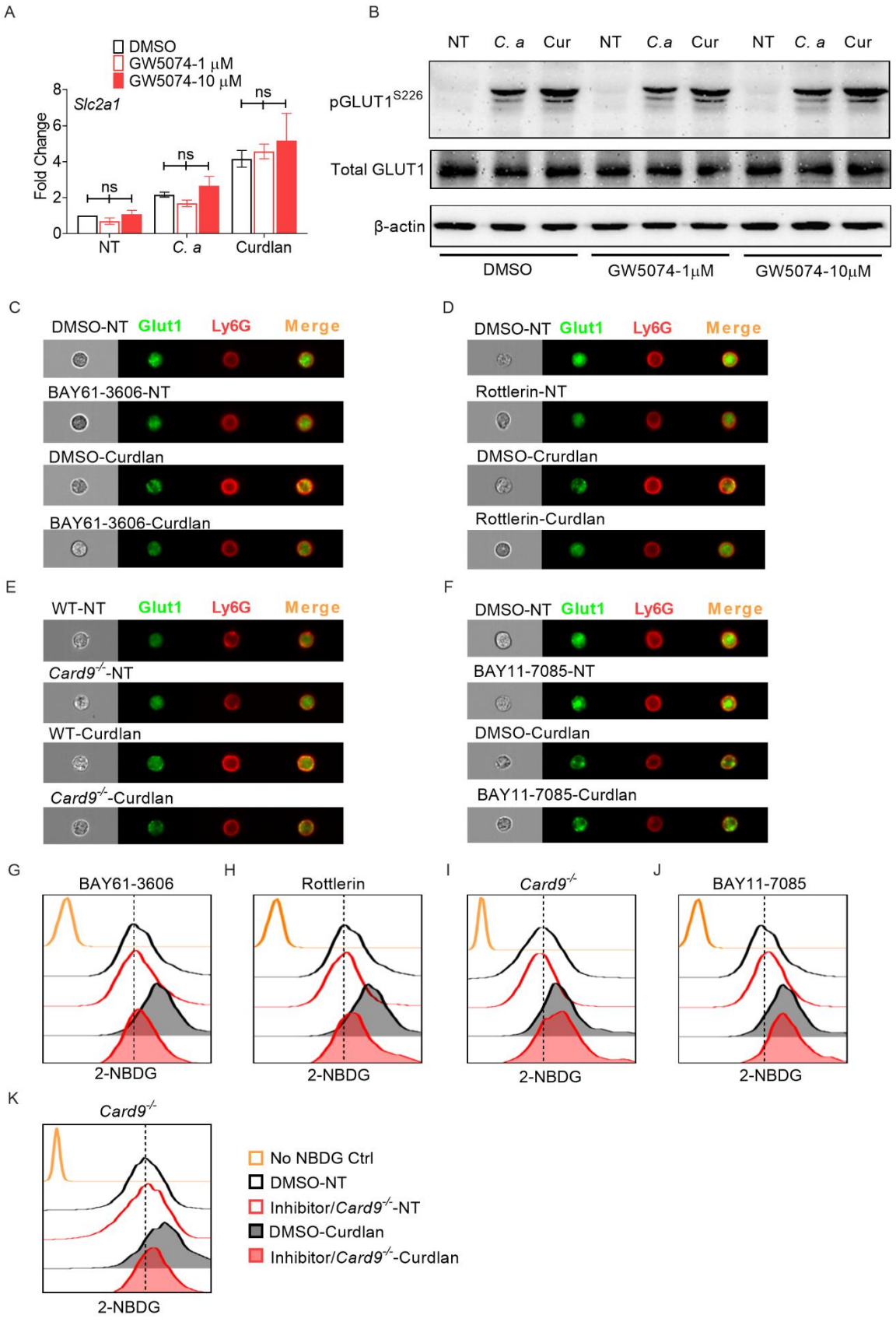
A
DMSO
GW5074-1 μM
GW5074-10 μM
Slc2a1
Fold Change
ns
NT
C. a
Curdlan
B
NT
C. a
Cur
pGLUT1S226
Total GLUT1
β-actin
DMSO
GW5074-1μM
GW5074-10μM
C
DMSO-NT
Glut1
Ly6G
Merge
BAY61-3606-NT
DMSO-Curdlan
BAY61-3606-Curdlan
D
Rottlerin-NT
DMSO-Crurdlan
Rottlerin-Curdlan
E
WT-NT
Card9-/--NT
WT-Curdlan
Card9-/--Curdlan
F
BAY11-7085-NT
BAY11-7085-Curdlan
G
BAY61-3606
H
Rottlerin
I
Card9-/-
J
BAY11-7085
2-NBDG
K
No NBDG Ctrl
DMSO-NT
Inhibitor/Card9-/--NT
DMSO-Curdlan
Inhibitor/Card9-/--Curdlan

Fig S2: Glut1 function is regulated by the dectin-1/PKCδ pathway in neutrophils. **(A)** BM neutrophils from WT mice were stimulated with *C. albicans (C. a)* (MOI=0.2) or curdlan (Cur) (10 μg/ml) for 3 h with/without Raf-1 inhibitor GW5074. Gene expression of *Slc2a1* was measured by qPCR, normalized to *Gapdh*. **(B)** Neutrophils from WT mice were stimulated with *C. a* (MOI=1) or curdlan (100 μg/ml) for 30 min in the presence or absence of Raf-1 inhibitor GW5074. Phosphorylation of Glut1 was assessed by western blot. Neutrophils from WT or *Card9*$^{-/-}$ mice were stimulated with curdlan (100 μg/ml) for 1.5 h in the presence or absence of indicated inhibitors. (**C, D, E, F**) Localization of Glut1 in neutrophils was visualized by ImageStream. (**G, H, I, J**) Glucose uptake of neutrophils (2-NBDG^{+} cells) was detected by flow cytometry analysis. (**K**) Neutrophils from WT or *Card9*$^{-/-}$ mice were stimulated with curdlan (10 μg/ml) for 6 h, and glucose uptake of neutrophils (2-NBDG^{+} cells) was detected by flow cytometry analysis. Data pooled from at least 3 independent experiments and representative images are shown. Statistical analysis by Two-way ANOVA (A). Data are represented as mean ± SEM (A). (Related to Figure 3 and 4)

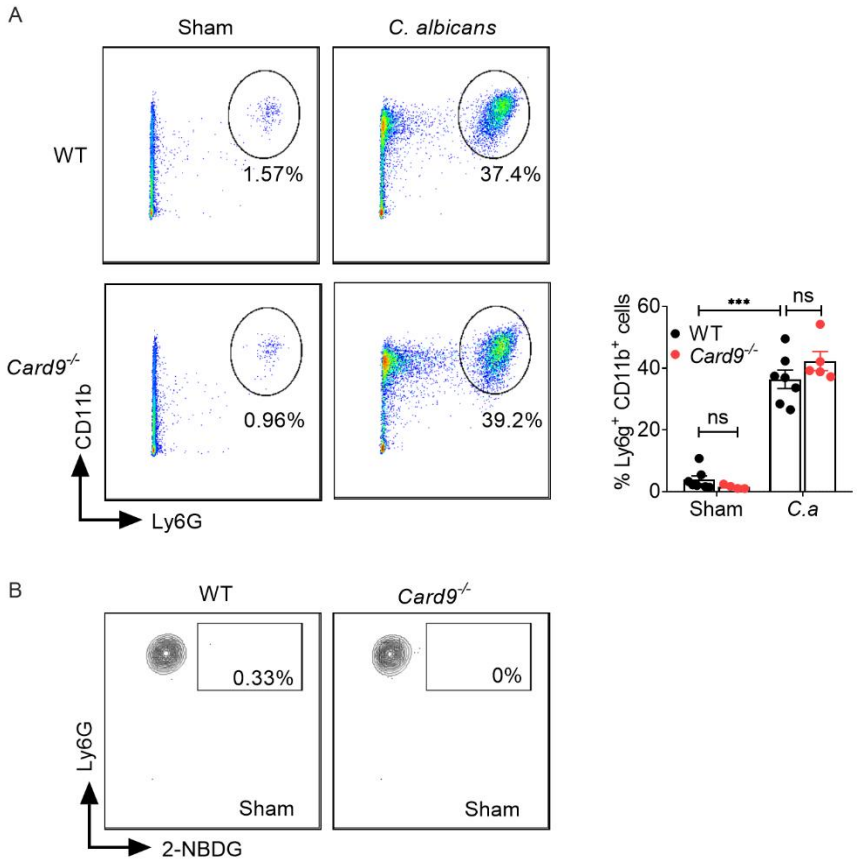

Fig S3: Card9$^{-/-}$ mice showed compromised glucose uptake after C. albicans infection. WT or *Card9*$^{-/-}$ mice were infected with 10^5 CFU of *C. albicans (C. a)* for 24 h (n=4-7). **(A)** The number of kidney-infiltrating neutrophils and (**B**) glucose uptake by neutrophils (2-NBDG$^+$ cells) were measured by flow cytometry analysis. Data pooled from at least 2 independent experiments and representative images are shown. Statistical analysis by Two-way ANOVA (A). Data are represented as mean ± SEM (A). (Related to Figure 4)

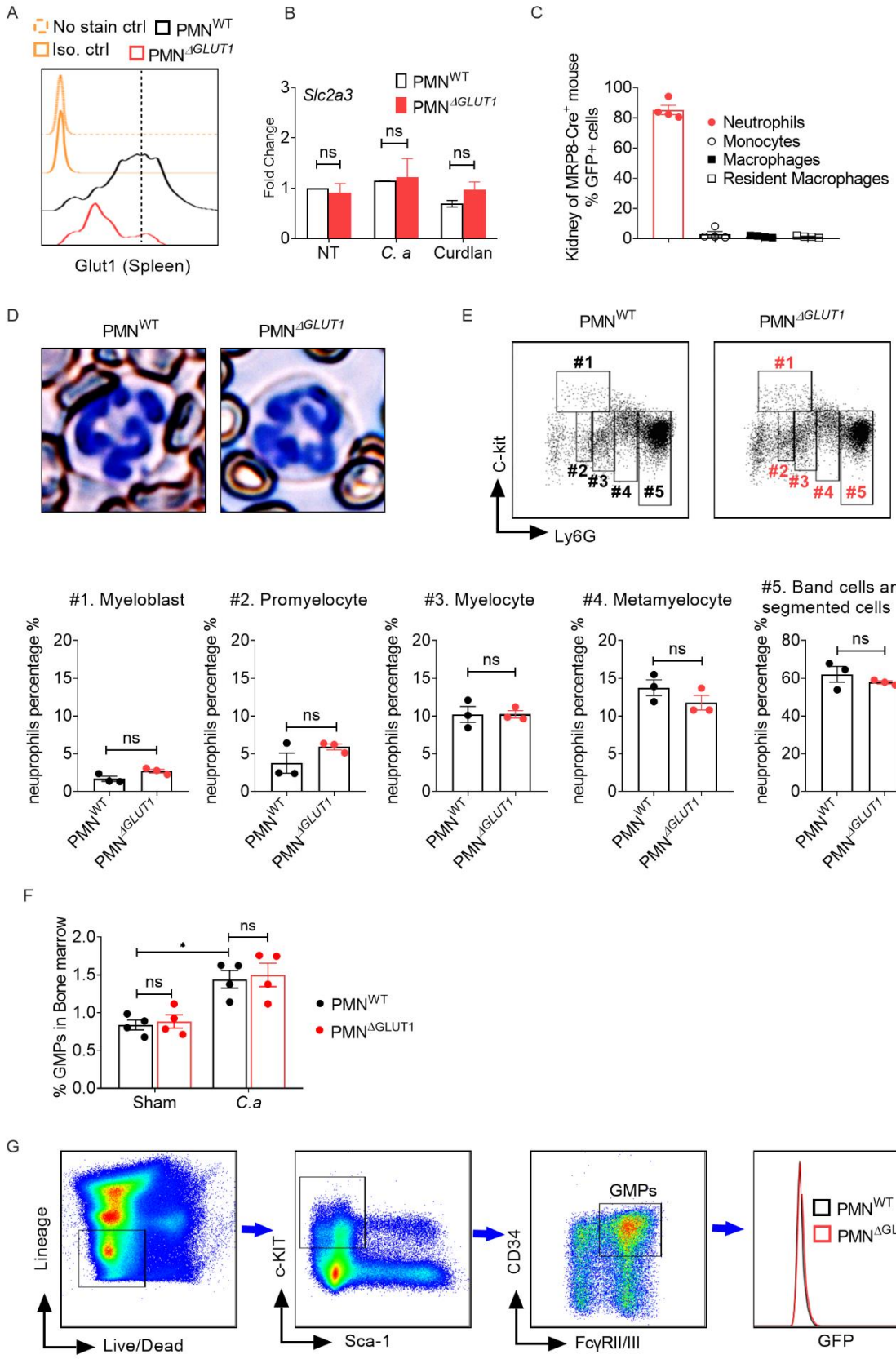
A
No stain ctrl
PMN^WT
Iso. ctrl
PMN^ΔGLUT1
Glut1 (Spleen)
B
Slc2a3
PMN^WT
PMN^ΔGLUT1
Fold Change
ns
NT
C. a
Curdlan
C
Kidney of MRP8-Cre+ mouse
% GFP+ cells
Neutrophils
Monocytes
Macrophages
Resident Macrophages
D
PMN^WT
PMN^ΔGLUT1
E
PMN^WT
PMN^ΔGLUT1
C-kit
Ly6G
#1
#2
#3
#4
#5
#1. Myeloblast
#2. Promyelocyte
#3. Myelocyte
#4. Metamyelocyte
#5. Band cells and segmented cells
neuprophils percentage %
F
% GMPs in Bone marrow
Sham
C.a
PMN^WT
PMN^ΔGLUT1
G
Lineage
Live/Dead
c-KIT
Sca-1
CD34
FcγRII/III
GMPs
GFP

Fig S4: Neutrophil-specific Glut1 conditional knockout mice exhibited normal granulopoiesis and neutrophil morphology. **(A)** Glut1 expression in the splenic neutrophils was measured by flow cytometry analysis**.** (**B**) BM neutrophils from PMN^{WT} or $PMN^{\Delta GLUT1}$ mice were stimulated with *C. albicans (C. a)* (MOI=0.2) or curdlan (Cur) (10 μg/ml) for 3 h. Gene expression of *Slc2a3* was measured by qPCR, normalized to *Gapdh*. (**C**) Neutrophils ($liveCD45^+CD11b^+Ly6G^+$), kidney-resident macrophages ($liveCD45^+Ly6C^+Ly6G^-CD11b^{hi}F4/80^{hi}CX3Cr1^+$) and monocyte/macrophages ($liveCD45^+Ly6C^+Ly6G^-CD11b^{low}F4/80^{low}$/$liveCD45^+Ly6C^+Ly6G^-CD11b^{hi}F4/80^{hi}$) were assessed for MRP8Cre activity on the basis of GFP expression by flow cytometry analysis at the baseline. **(D)** Peripheral blood smears of PMN^{WT} and $PMN^{\Delta GLUT1}$ mice were stained with Giemsa stain and microscopically evaluated for the morphology of neutrophils. **(E)** Granulopoiesis in the BM of PMN^{WT} and $PMN^{\Delta GLUT1}$ mice was measured by flow cytometry analysis. BM of PMN^{WT} and $PMN^{\Delta GLUT1}$ mice were evaluated for **(F)** frequency of GMPs before and after infection and **(G)** MRP8Cre activity at the baseline by flow cytometry analysis. Representative flow cytometry analysis plots from 1 of 3-4 mice were shown (E-G). Data pooled from at least 2 independent experiments (A-G) and representative images are shown. Statistical analysis by Two-way ANOVA (B and F) or Student's T test (E). Data are represented as mean ± SEM (B, C, E, F). (Related to Figure 5)

A

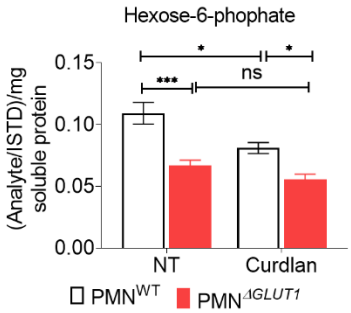
Hexose-6-phophate
(Analyte/ISTD)/mg soluble protein
0.15
0.10
0.05
0.00
*
***
ns
*
NT
Curdlan
PMN^WT
PMN^ΔGLUT1

B

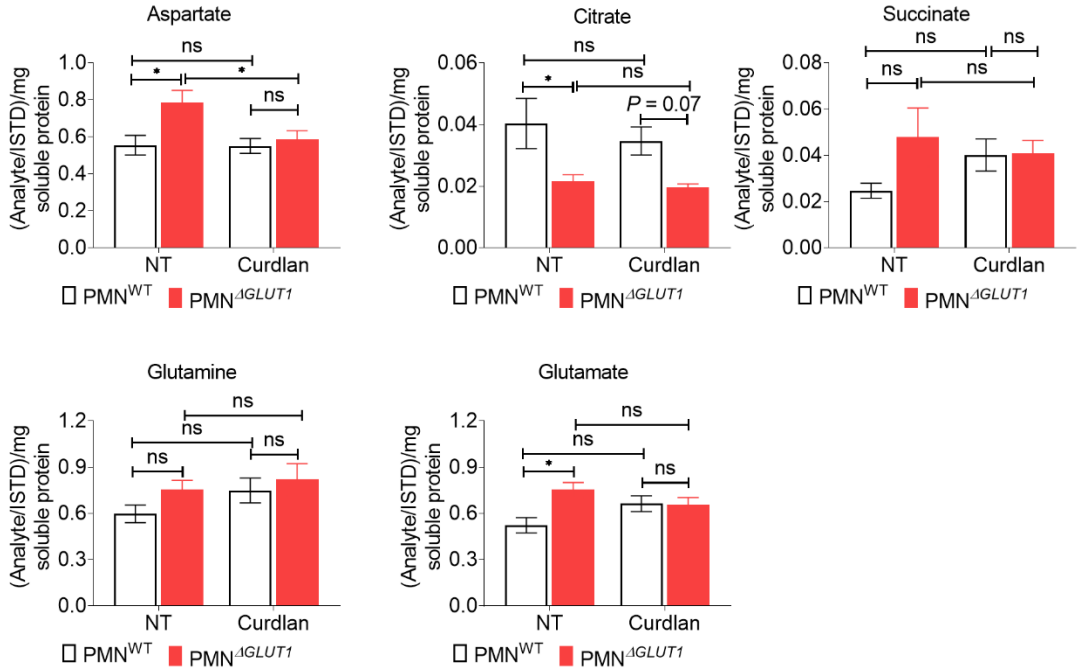
Aspartate
Citrate
Succinate
Glutamine
Glutamate
(Analyte/ISTD)/mg soluble protein
ns
*
P = 0.07
NT
Curdlan
PMN^WT
PMN^ΔGLUT1

C

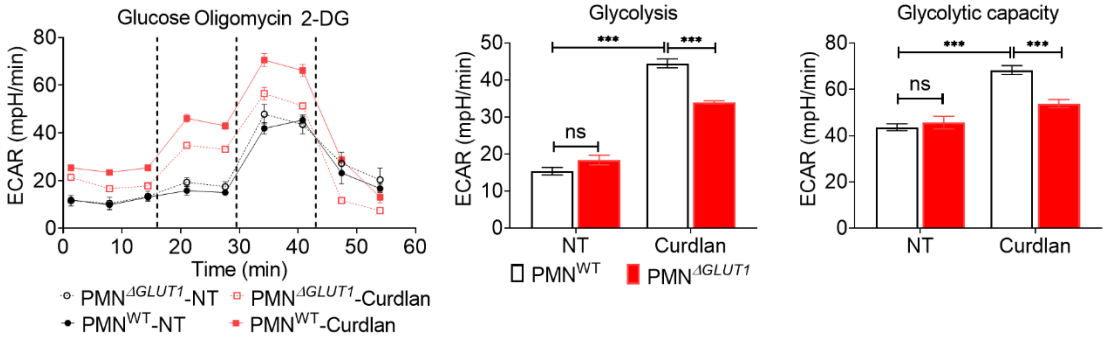
Glucose Oligomycin 2-DG
ECAR (mpH/min)
Time (min)
PMN^ΔGLUT1-NT
PMN^ΔGLUT1-Curdlan
PMN^WT-NT
PMN^WT-Curdlan
Glycolysis
Glycolytic capacity
***
ns
NT
Curdlan
PMN^WT
PMN^ΔGLUT1

Fig S5: Glut1 deficiency in neutrophils suppresses glycolysis after curdlan stimulation. BM neutrophils from PMN^{WT} or $PMN^{\Delta GLUT1}$ mice (n=8) were stimulated with curdlan (Cur) (10 μg/ml) for 3 h. Cell pellets were subjected to a metabolomics study using untargeted LC-HRMS. **(A)** Hexose-6-phophate and **(B)** metabolites of TCA cycle expression between before and after curdlan stimulation were detected using untargeted high-resolution LC-HRMS. (**C**) BM neutrophils from PMN^{WT} and $PMN^{\Delta GLUT1}$ mice were stimulated with curdlan (10 μg/ml) for 3 h. Seahorse assay was performed to detect the ECAR (Basal extracellular acidification rate) before and after curdlan stimulation. Data pooled from 3-4 independent experiments. Statistical analysis by Two-way ANOVA (A-C). Data are represented as mean ± SEM (A-C). (Related to Figure 5)

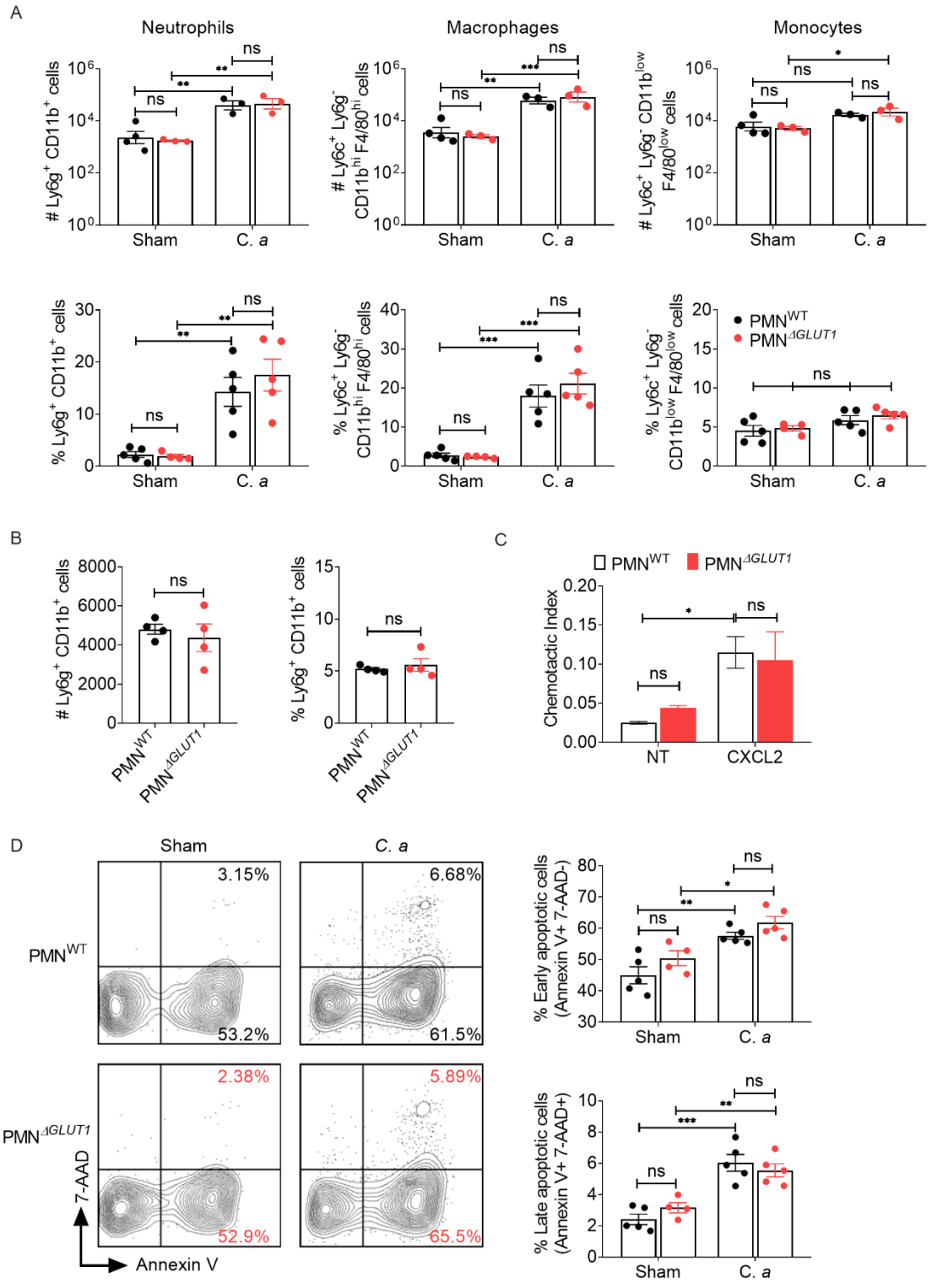
A
Neutrophils
Macrophages
Monocytes
Ly6g+ CD11b+ cells
Ly6c+ Ly6g- CD11bhi F4/80hi cells
Ly6c+ Ly6g- CD11blow F4/80low cells
% Ly6g+ CD11b+ cells
% Ly6c+ Ly6g- CD11bhi F4/80hi cells
% Ly6c+ Ly6g- CD11blow F4/80low cells
Sham
C. a
ns
PMNWT
PMNΔGLUT1
B
Ly6g+ CD11b+ cells
% Ly6g+ CD11b+ cells
C
Chemotactic Index
NT
CXCL2
D
Sham
C. a
PMNWT
PMNΔGLUT1
3.15%
53.2%
6.68%
61.5%
2.38%
52.9%
5.89%
65.5%
7-AAD
Annexin V
% Early apoptotic cells (Annexin V+ 7-AAD-)
% Late apoptotic cells (Annexin V+ 7-AAD+)

Fig S6: Deficiency of Glut1 in neutrophils has no impact on migration and apoptosis. PMN^{WT} and $PMN^{\Delta GLUT1}$ mice were infected with 10^5 CFU of *C. albicans (C. a)* for 24 h. **(A)** Number of kidney-infiltrating neutrophils, macrophages and monocytes were detected by flow cytometry analysis. **(B)** PMN^{WT} and $PMN^{\Delta GLUT1}$ mice were infected with 5 x 10^6 CFU of *C. albicans (C. a*) for 2 h. Kidney infiltrating neutrophils were detected by flow cytometry analysis. **(C)** BM neutrophils from PMN^{WT} and $PMN^{\Delta GLUT1}$ mice were subjected to transwell migration assay in the presence or absence of of recombinant murine CXCL2 (100 ng/ml) for 1.5 h. The numbers of neutrophils in the lower and upper chambers were quantified by flow cytometry analysis and expressed as Chemotactic Index. **(D)** PMN^{WT} and $PMN^{\Delta GLUT1}$ mice were infected with 10^5 CFU of *C. a* for 24 h. Apoptosis of kidney infiltrating neutrophils was detected by flow cytometry analysis. Data pooled from at least 2 independent experiments and representative images are shown in D. Statistical analysis by Two-way ANOVA (A, C, D) or Student's T test (B). Data are represented as mean ± SEM (A-D). (Related to Figure 6)

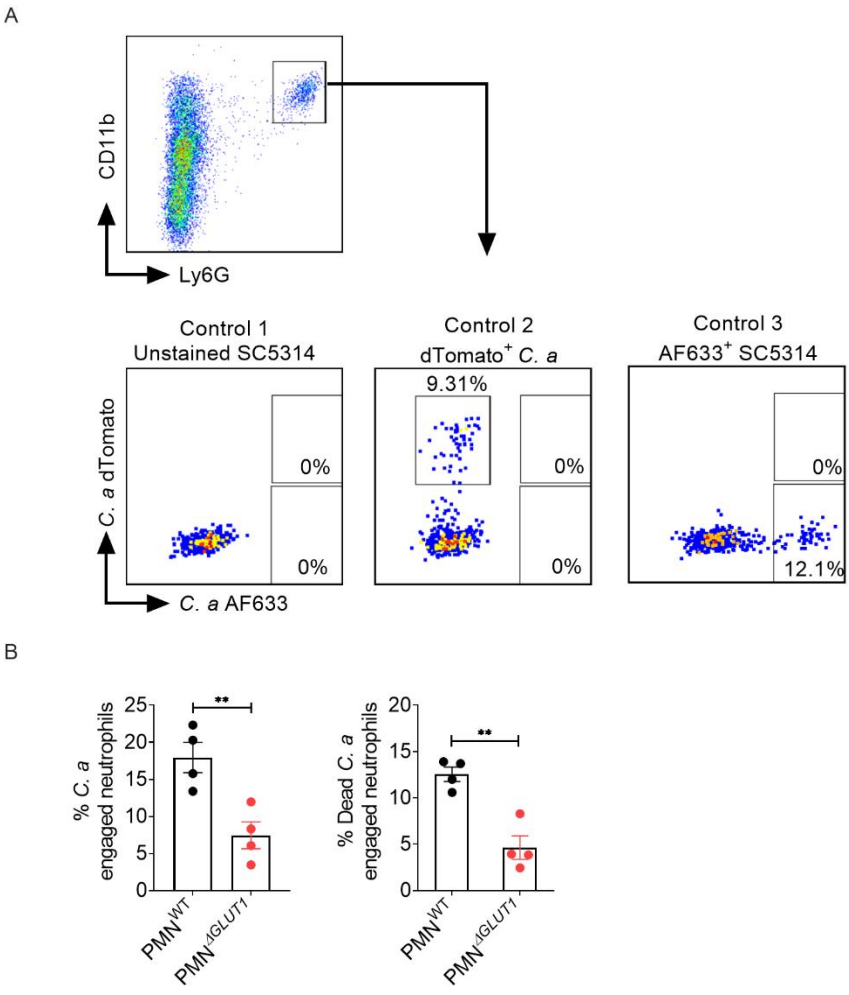

Fig S7: Deficiency of Glut1 impaired phagocytosis and intracellular killing by neutrophils in C. albicans infection. **(A)** WT mice were infected with 5 x 10^6 CFU of *C. albicans (C. a)* (Control 1) or dTomato$^+$ *C. a* (Control 2) or AF633$^+$ *C. a* (Control 3). Mice were sacrificed at 2 h p.i. and phagocytosis and intracellular killing by kidney infiltrating neutrophils were measured by flow cytometry analysis. **(B)** PMN^{WT} and PMN$^{\Delta GLUT1}$ mice were infected with 5 x 10^6 CFU of Streptavidin-AF633$^+$dTomato$^+$ *C. a*. Mice were sacrificed at 2 h p.i. and phagocytosis and intracellular killing by kidney-infiltrating neutrophils were measured by flow cytometry analysis. Percentage of *C. a* engulfed neutrophils and percentage of dead *C. a* engulfed neutrophils are

shown. Data pooled from at least 2 independent experiments and representative images are shown in A. Statistical analysis by Student's T test (B). Data are represented as mean ± SEM (B). (Related to Figure 6)

Supplementary Table 1: Demographic information of healthy volunteers (n=10) (Related to Figure 7 and STAR Methods)

Total number of human subjects	**Race**	**Gender**	**Age**
10	7 Asians 2 African Americans 1 Caucasian	9 Males 1 Female	32.1 ± 7.1

Supplementary Table 2: Oligonucleotides used in this study. (Related to STAR Methods)

Oligonucleotides	**Source**	**Identifier**
Mm_Slc2a1_1_SG QuantiTect Primer Assay	QIAGEN	Cat# QT01044953
Mm_Slc2a2_1_SG QuantiTect Primer Assay	QIAGEN	Cat# QT00103537
Mm_Slc2a3_1_SG QuantiTect Primer Assay	QIAGEN	Cat# QT00159691
Mm_Slc2a4_1_SG QuantiTect Primer Assay	QIAGEN	Cat# QT01044953
Mm_Slc2a7_1_SG QuantiTect Primer Assay	QIAGEN	Cat# QT00323057
Mm_Slc2a8_1_SG QuantiTect Primer Assay	QIAGEN	Cat# QT00119602
Mm_Slc2a9_1_SG QuantiTect Primer Assay	QIAGEN	Cat# QT00106785
Mm_Slc2a10_1_SG QuantiTect Primer Assay	QIAGEN	Cat# QT00252553
Mm_Slc2a12_1_SG QuantiTect Primer Assay	QIAGEN	Cat# QT00173719
Mm_Gapdh_3_SG QuantiTect Primer Assay	QIAGEN	Cat# QT01658692
Hs_SLC2A1_1_SG QuantiTect Primer Assay	QIAGEN	Cat# QT00068957
Hs_GAPDH_1_SG QuantiTect Primer Assay	QIAGEN	Cat# QT00079247